Desalination and Water Treatment
www.deswater.com

doi:10.5004/dwt.2017.20801

79 (2017) 273–281
June

Mixture of illite-kaolinite for efficient water purification: Removal of As(III) from aqueous solutions

Omer Sakin Omer[a,b], Belal H.M. Hussein[a,c], Mohammed Ali Hussein[b], Arbi Mgaidi[a,*]

[a]*Chemistry Department, Faculty of Sciences and arts, Al Ula Branch, Taibah University,Saudi Arabia, Tel.+966595241830, email: omsakin@gmail.com (O.S. Omer), Tel. +9665327705025, email: Belalhussein102@yahoo.com (B.H.M. Hussein), Tel. +966546834407, email: amgaidi@taibahu.edu.sa (A. Mgaidi)*
[b]*Department of Industrial and Applied Chemistry, Faculty of Pure and Applied Science, International University of Africa, Sudan, Tel. +249912211641, email: moalhu01@gmail.com (M.A. Hussein)*
[c]*Department of Chemistry, Faculty of science, Suez Canal University, Ismailia, Egypt*

Received 6 December 2016; Accepted 10 April 2017

ABSTRACT

Adsorption technology is one of the most promising technologies to remove heavy metals from water. This paper aims to remove arsenite As(III) from contaminated water using a less costly, easier to handle and efficient absorbent. Purified natural clay was characterized and tested as an adsorbent. Mineralogical and textural analysis showed that this adsorbent is a nonswelling clay mineral (illite + kaolinite) and a mesoporous material with specific surface area S_{BET} = 128 $m^2 \cdot g^{-1}$. A series of batch tests were performed as a function of contact time (10–180 min), temperature (25–55°C), initial As(III) concentration (20–100 $mg \cdot L^{-1}$) and solid/liquid ratio (5–25 $g \cdot L^{-1}$). The adsorption equilibrium studies revealed that Freundlich isotherm was followed with a better correlation than the Langmuir isotherm, moreover, it was intra particle diffusion controlled. The adsorption of As(III) onto the mixture illite-kaolinite was significant in the pH range 9–10.8 with a maximum adsorption capacity q_{max} = 233.1 $mg \cdot g^{-1}$. At 298 K, the thermodynamic investigation indicates that the adsorption processes is spontaneous ($\Delta G°_{ads}$ = –9.3 $kJ \cdot mol^{-1}$) and exothermic ($\Delta H°_{ads}$ = –4.58 $kJ \cdot mol^{-1}$). The $\Delta S°_{ads}$ parameter was found to be +15.8 $J \cdot mol^{-1} \cdot K^{-1}$ meaning an increase in the randomness of the processes at the surface of clay particles.

Keywords: Illite/kaolinite clay minerals; Arsenite adsorption; Freundlich and Langmuir models; Intra particle diffusion; Thermodynamics

1. Introduction

In Africa and especially in Sudan, groundwater is one of the major sources of drinking water. Unfortunately, this water may be contaminated by heavy metals such as arsenic which is the most dangerous pollutants [1].

World Health Organization (WHO) have lowered the provisional guideline for As in public water to 10 $\mu g \cdot L^{-1}$ [2]. Arsenic contaminated water contains arsenous acid H_3AsO_3 and arsenic acid H_3AsO_4 or their derivatives. Arsenite As(III) is more dangerous and more difficult to remove from drinking water than pentavalent arsenate As(V) [3]. So, the literature review showed that removal of the As(V) from water was more studied than As(III) using different low-cost absorbents [4].

Several techniques for the removal of As from water are available; including reverse osmosis, ion-exchange, coagulation/precipitation, adsorption etc. Each process has its own merits and demerits such as the operational high costs. Adsorption still remains an attractive and promising technology, because of its simplicity, ease of operation and handling. Natural clays and their modified forms have received more attention for use as an adsorbent in removing water pollutants such as arsenic ions (As(III) and As(V)) [5].

In 1988, natural China clay with S_{BET} = 13.5 $m^2 \cdot g^{-1}$ was used to remove arsenite from aqueous solutions [6].

*Corresponding author.

Maximum removal was found to be 0.023 mg·g^{-1} at pH = 8 after 3H of contact time. In another study, maximum removal reached 75 mg·g^{-1} when a natural clay, composed of 80% smectite and 20% illite with S_{BET} = 158 m^2·g^{-1} (43% of porosity) was tested for removal of arsenite(III) from water at 298K and pH range 3–9 [7].

Natural laterite (rock type rich in iron and aluminum) was used as an adsorbent for As(III) removal with as maximum efficiency about 98% at S/L = 4/100 and $[As^{3+}]_0$ = 1 mg·L^{-1} [8]. Sepiolite which is a non-swelling, lightweight and porous clay mineral with S_{BET} = 300 m^2·g^{-1} was investigated to remove As(III) from groundwater [9]. The results of this study showed that when the absorbent was iron oxide-coated its maximum adsorption capacity had reached 0.309 mg·g^{-1}. Arsenite(III) adsorption on natural side rite (iron(II) carbonate $FeCO_3$), achieved equilibrium at 24 h with maximum adsorption capacity (q_m) = 9.43 mg·g^{-1} [10]. The differences in the maximum adsorption capacities of natural clays could be attributed to the following parameters: iron content, specific surface area S_{BET} and average pore diameter [11]. The acid- activated montmorillonite (swelling clay mineral type 2/1) with high S_{BET} 140 m^2·g^{-1} has a maximum adsorption capacity equal to 159.43 mg·g^{-1} for As(III) at fixed pH = 5. However naturally monmorillonite (S_{BET} 32 m^2·g^{-1}) has a maximum adsorption capacity for As(III) equal to 10.34 mg·g^{-1} [5]. The Ti-pillared montmorillonite (S_{BET} 164.6 m^2·g^{-1} and average pore diameter 1.76–2.76 nm) had a maximum adsorption capacity of about 16 mg·g^{-1}, when tested to remove As(III) from drinking water at optimum pH within the range 4–10 [12]. Synthesized and calcined 2:1 clay type-an alumina octahedral sheet sandwiched between two silica tetrahedral sheets-was found to has a higher maximum adsorption capacity of 295 mg·g^{-1} for As(III) removal from aqueous solutions [13], but unfortunately, the adsorption process was slow, it took 20 h to reach the equilibrium state.

Authors noted that competing anions strongly affected the adsorption of As(III) onto clay when the clay contains about 10% iron (Vermiculite) the maximum adsorption capacity of arsenite, at pH = 5 and T = 293 K, had reached 72.2 mg·g^{-1} after 30 min of contact time [14].

The present paper aims to investigate natural, modified and low cost clay as an absorbent to remove arsenite from aqueous solutions under different parameters (initial concentration of As^{3+} ions, temperature and adsorbent dose). After characterization of the adsorbent used, modelling of kinetic data and thermodynamic behavior were carried out to reach more insight into the adsorption process.

2. Materials and methods

2.1. Preparation of the adsorbent

Raw clay sample was purchased from Almarwani for Spices Company, Saudi Arabia. Due to its wide dispersion and easy separation, the raw clay was converted to its sodium form by ion exchange process with sodium chloride [15]. Certain amount of the clay was suspended in 1 M NaCl solution with 5% clay to solution ratio, and agitated for 12 h using mechanical stirrer, Heidolph instruments type RZR 1, Germany. The Na-clay was separated from the solution by centrifugation for 10 min at 5000 rpm using EBA 20 centrifuge Hettich Type. The process repeated several times. Excess chloride was washed out repeatedly with double distilled water and the supernatant was tested for excess chloride by a simple silver nitrate test. The modified clay was then dried in an oven for 72 h at 60ºC, ground and sieved to obtain a fine texture.

2.2. Adsorbent characterization

The Na-clays were characterized by a powder X-ray diffractometer (Phillips Xpert-pro) between 5° and 60° 2θ using Cu K_α radiation. The microstructure of the adsorbent was investigated using a JEOL JED2200 series coupled with an energy dispersive X-ray detector (SEM/EDS). Fourier Transform Infrared (FTIR) spectra in the region 4000–400 cm^{-1} were investigated using Thermo Scientific spectrometer with DTGS detector and a KBr splitter. The KBr pressed disc technique (1 mg of sample and 200 mg of KBr) was used. Spectra manipulations were performed using the OMNIC software package (Thermo Instruments Corp.). The specific surface areas and pore size distribution were estimated by N_2 physisorption at 77 K with the application of the Brunauer–Emmet–Teller (BET) equation on a Micromeritics ASAP2000 apparatus. The sample was degassed at 373 K prior to BET measurements during 1H. Thermo gravimetric analysis (TGA/DTG) was performed with a SETRAM type 124 TG/DTA instrument using aluminum as inert reference material. The temperature was increased from room temperature to 900°C at the regular increment of 10°C/min in the air atmosphere.

2.3. Reagents and Instrumentals

A stock solution of arsenite 1g·L^{-1} was prepared from $NaAsO_2$ salt provided by Fine Chemical, UK (purity >99%). Different solutions in the concentration range 20–100 mg·L^{-1} of As(III) were prepared using deionized water by dilution from the stock solution. The concentration of As(III) was measured using Inductively Coupled Plasma ICP (Perkin Elmer instrument) at wavelength 228 nm calibrated using standard diluted As(III) solutions.

2.4. Batch adsorption experiments

Our adsorption experiments were carried out by a batch process. Twenty five milliliters of aqueous solution at the desired initial concentration was mixed with 0.125 to 0.625 g of clay at initial pH about 7.5.

The effect of temperature for As(III) adsorption on the Illite-kaolinite clay was studied in 50 mL Erlenmeyer flasks containing 25 mL of synthetic arsenite solution (20 mg/L) and S/L ratio = 0.5. The Samples were shaken using shaker incubator model LSI-100B from KWF Sci-Tech & development Co. The temperatures were 298, 308, 318 and 328 K.

The adsorption capacity of As(III) at equilibrium, (q_e, mg·g^{-1}), was calculated according to Eq. (1):

$$q_e = \frac{(C_0 - C_e)V}{m} \quad (1)$$

where q_e is the amount of As(III) adsorbed per unit weight of clay in (mg·g^{-1}), C_e is the equilibrium concentration of

As(III) in (mg·L^{-1}), C_0 is the initial metal ion concentration in (mg·L^{-1}), V is the volume of solution in (L) and m is the dry weight of the clay in (g).

3. Results and discussion

3.1. Characterization of adsorbent

3.1.1.XRD analysis

Fig. 1 shows the diffraction results of the adsorbent used. The *d*-spacing observed at 10.42 and 7.12 Å are typical for illite and kaolinite respectively and agree well with those reported in the literature [2]. In this figure, we can also see a peak of quartz at d = 4.46. According to this mineralogical analysis, we can state that the clay is naturally composed of illite associated with kaolinite and quartz.

3.1.2. Morphological characterization of the adsorbent

The SEM image of the adsorbent studied in this work is shown in Fig. 2. A perfect cleavage can be observed (see Fig. 2a). From Fig. 2b, we can observe that the surface morphology appeared to possess an irregular texture and porous cavities depending on the pore size and diameter of the absorbent and ionic size and diameter of the soluble forms of As(III) which are available sites for As(III) adsorption. The qualitative chemical analysis showed an aluminum silicate mineral with amounts of Fe and Mg (Fig. 2c).

3.1.3. Textural properties

As it can be seen in Fig. 3 the N_2 adsorption desorption isotherms exhibit type IV isotherms with H3 type hysteresis loop. This type is characteristic of relatively large pores (about 50 nm mesopores with capillarity condensation mechanism).

The pore size distribution was calculated using the Kelvin equation as a relationship between the vapor relative pressure and the pore radius (Barret-Joyner-Halenda analysis BJH). The pore size distribution depicted in Fig. 4 are typical for materials which have slit-shaped pores.

As it can be seen from this figure, the clay shows a pore size distribution in the mesopores range (5–50 nm) with a significant contribution of pores around 40 nm of diameter. Textural parameters of the adsorbent are summarized in Table 1.

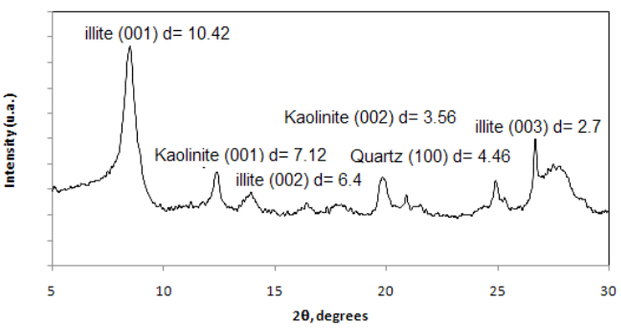

Fig. 1. X-ray diffraction (XRD) pattern of the clay used.

3.1.4. FT-IR analysis

Fig. 5 shows the FT-IR spectrum of the clay used in this study. Kaolinite Si–O stretching vibration appeared at 798 cm^{-1}. Adsorption bands at 794 cm^{-1} and 912 cm^{-1} are also attributable to kaolinite [2]. For illite, a peak at 3620 cm^{-1} is observed which is due to the inner-surface OH groups located on the surface of the octahedral sheet between 2 layers. The vibration of adsorbed water appeared at 3420 cm^{-1} and for the hydration water at 1640 cm^{-1}.

3.1.5. Thermal analysis

The thermal decomposition of the adsorbent used in this work was investigated with the thermogravimetric (TG) and differential thermogravimetric analysis (DTA). Results are reported in Fig. 6. Three stages of mass loss are observed. The first loss can be assigned to the loss of a small percent (2.7%) of adsorbed water in the bulk of clay particles in the channels that are attached to the sides of the silicate units. The loss of such adsorbed water is more gradual and may persist continuously to a temperature higher than 100–150°C. The following losses were the lower range dehydroxylation (450–600°C) and higher dehydroxylation (600–900°C), respectively. The lower and higher dehydroxylation temperature ranges (450–900); represent the formation of metakaolinite phase [2–7].

3.2. Adsorption isotherms

The Langmuir and Freundlich isotherms are the most common isotherm models, used to describe physical adsorption in a solid-liquids system. The Langmuir equation is defined as follows:

$$q_e = \frac{K_L q_{\max} C_e}{1 + K_L C_e} \tag{2}$$

where q_{max} is the maximum adsorption capacity of the adsorbent (mg·g^{-1}) and K_L (L·mg^{-1}) is the Langmuir adsorption constant related to the binding energy of adsorption [10].

The Freundlich model is defined by:

$$q_e = k_F C_e^{1/n} \tag{3}$$

where k_F is the Freundlich constant indicating the relative adsorption capacity for the adsorbent, and *1/n* is the heterogeneity factor indicating the adsorption intensity [10].

Both Eqs. (2) and (3) with two adjustable parameters were numerically solved using the solver program of Microsoft Excel with Newton method.

The mean square error (MSE, objective function) used was based on the relative deviation between the experimental value $q_{e,exprimental}$ and the theoretical value $q_{e,model}$ and calculated from Eq. (4):

$$MSE = \sum_{i=1}^{N} \left(\frac{q_{e,\text{experimental}} - q_{e,\text{model}}}{q_{e,\text{experimental}}} \right)^2 \tag{4}$$

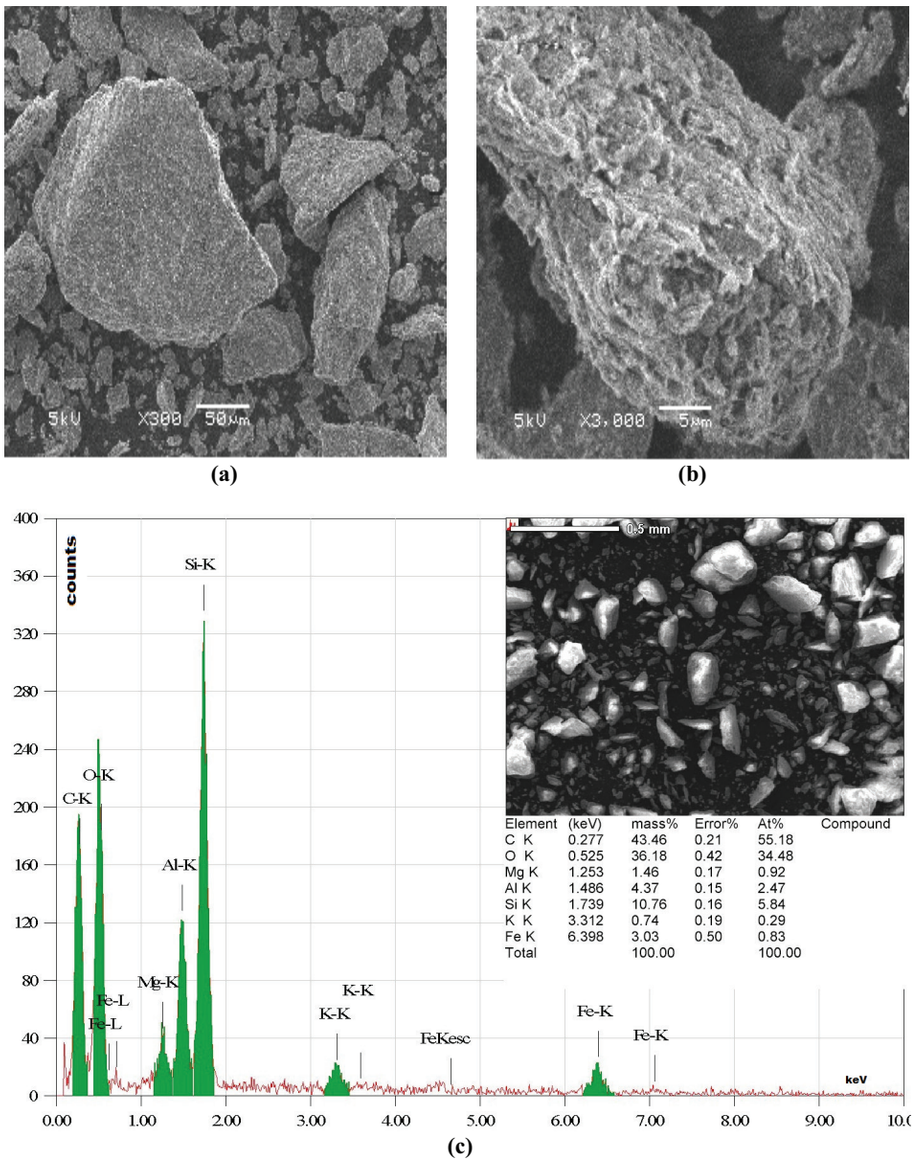

Fig. 2. Surface morphology and EDS analysis of the clay used.

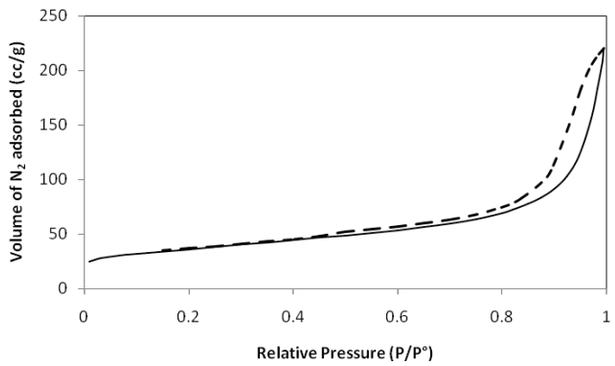

Fig. 3. N_2 adsorption-desorption isotherms and pore size distribution of green clay used.

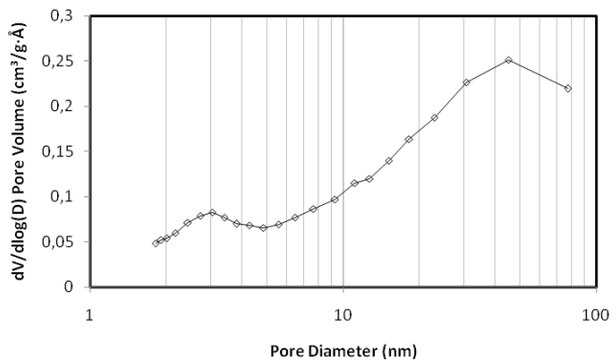

Fig. 4. Pore size distribution of the clay as determined by the BJH method.

Table 1
Textural parameters of the studied adsorbent

Property	S_{BET} (m^2/g)	BJH surface (m^2/g)	Single point surface Area at $p/p° = 0.2$ (m^2/g)	Total pore volume (cm^3/g)	Average pore size by BET (Å)	Average pore size by BJH (Å)
Value	128	86	126	0.320	75.6	148.0

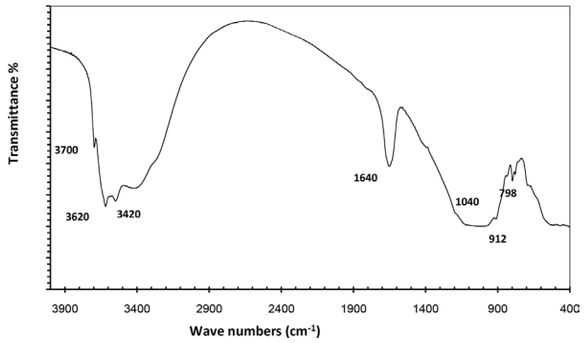

Fig. 5. FTIR spectrum of clay used.

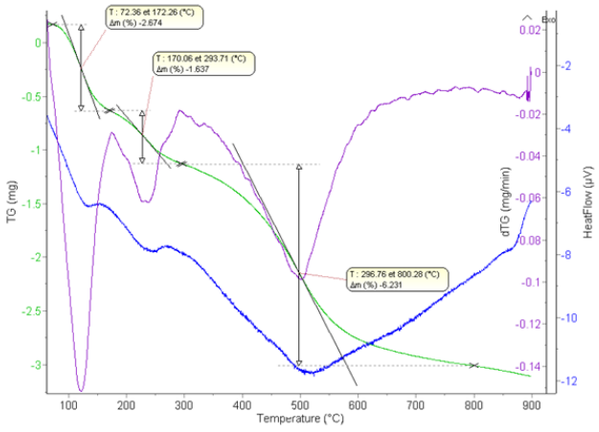

Fig. 6. TG-DTA thermogram for the starting material.

The root mean square error (RMSE, percentage deviation) function was calculated for the different models using Eq. (5):

$$\%\mathrm{RMSE} = \sqrt{\frac{1}{N-m}\sum_{i=1}^{N}\left(\frac{q_{e,\mathrm{experimental}} - q_{e,\mathrm{model}}}{q_{e,\mathrm{experimental}}}\right)^2} \times 100 \qquad (5)$$

where N is the number of experimental points and m is the number of identified parameters. Eq. (5) indicates the performance of the best fit between the experimental and predicted curves.

A comparison between the experimental amount of As(III) adsorbed per unit weight of clay and the simulated data using Langmuir or Freundlich isotherms is shown in Fig. 7.

Results in Fig. 7 showed that Freundlich model fitted As(III) adsorption data at different solid to liquid ratios

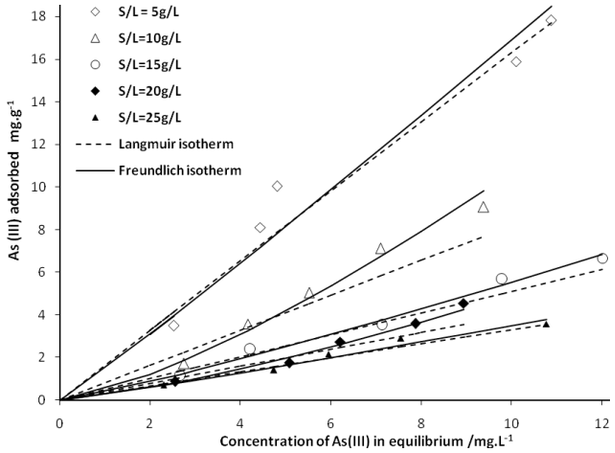

Fig. 7. Equilibrium isotherm plots for As(III) onto illite + kaolinite at a different ratio (solid/liquid 5–25 g·L^{-1}; T = 308 K and $[As^{3+}]_0$ = 20 mg·L^{-1}) (Langmuir isotherm: dashes lines and Freundlich isotherm: solid lines).

(S/L) better than Langmuir isotherm model. The obtained parameters (q_{max}, K_L, k_F and n) and root mean square deviation for each S/L ratio are summarized in Table 2. When the value of the parameter n is greater than unity that indicates the existence of repulsive forces between sorbed molecules [11]. From Table 2, we note that n values are less than unity and RMSE values of Freundlich equation were lower than Langmuir model. This might be due to the heterogeneous distribution of active sites on the clay surface.

3.3. Thermodynamic parameters

To calculate the thermodynamic parameters, we use the following equation:

$$\Delta G° = -RT \ln K^0 \qquad (6)$$

where $K°$ is the standard equilibrium constant which is a dimensionless parameter, but the units of $\Delta G°$, R and T are J·mol^{-1}, J·mol^{-1}·K^{-1} and K respectively. $K°$ is related to the constant ($k_d = q_e/C_e$) and the standard equilibrium constant could be calculated as [16,17]:

$$K° = \frac{q_e}{c_e} \times M_{Adsorbate} \times C^0 \qquad (7)$$

where M is the molecular weight of species adsorbed, $C°$ is the concentration of the solution in the chosen standard state ($C°$ = 1 mol·L^{-1}). Then:

Table 2
Isotherm parameters for As(III) adsorption onto Illite-kaolinite at different solid/liquid ratios S/L (5–25 g·L^{-1}) and T = 308 K and $[As(III)]_0$ = 20 mg·L^{-1}

Parameter	q_{max} (mg·g^{-1})	K_L (L·mg^{-1}) × 10^5	k_F (mg$^{1-1/n}$g^{-1}L$^{1/n}$)	n	RMSE Langmuir	RMSE Freundlich
S/L=5 g·L^{-1}	233.1	704	1.492	0.948	0.18	0.17
S/L=10 g·L^{-1}	233.1	353	0.472	0.737	0.24	0.09
S/L=15 g·L^{-1}	233.2	220	0.397	0.873	0.15	0.09
S/L=20 g·L^{-1}	233.3	171	0.235	0.757	0.21	0.11
S/L=25 g·L^{-1}	233.2	142	0.283	0.914	0.12	0.10

$$LnK° = -\frac{\Delta H°}{RT} + \frac{\Delta S°}{R} \quad (8)$$

and

$$\Delta S° = \frac{\Delta H° - \Delta G°}{T} \quad (9)$$

The $\Delta H°$ value was determined from the slope of the linear plot of Eq. (8), as shown in Fig. 8.

The values of thermodynamic parameters determined in this work are reported in Table 3.

$\Delta G°$ decreases with increasing temperature The negative $\Delta G°$ values indicate that the adsorption process is thermodynamically favorable and spontaneous. According to the value of $\Delta H°$ (negative), the adsorption of arsenite is an exothermic process. However, the positive value of $\Delta S°$ corresponds to the increasing randomness at the interface clay-arsenite solution and indicates the high affinity of illite + kaolinite for As(III). Also, it suggests some structural changes in the arsenic types. For example, in natural water, the major arsenite species are H_3AsO_3, $H_2AsO_3^-$, $HAsO_3^{2-}$ [9]. In acidic medium, the adsorption of As(III) is not favorable [18]. Fig. 9 shows the speciation of arsenite (III) as function of the pH of the solution [4]. In the pH range 0–9, the adsorbed species is mainly the H_3AsO_3 but at pH range 10–11, the anionic form $H_2AsO_3^-$ predominates. All our experimental sets were conducted in this range.

The interaction of arsenite species on clay surface can be described schematically as follows[8]:

$$\equiv MOH + H_3AsO_3 \rightarrow \equiv MH_2AsO_3 + H_2O \quad (10)$$

$$2\equiv MOH + H_3AsO_3 \rightarrow [\equiv MHAsO_3M\equiv] + 2H_2O \quad (11)$$

$$\equiv MOH_2^+ + H_2AsO_3^- \rightarrow \equiv MH_2AsO_3 + H_2O \quad (12)$$

where ≡MOH represents a reactive surface hydroxyl and M represents Si or Al/Fe. Eq. (10) represents monodentate ligand exchange and Eq. (11) the bidentate step. Whereas, Eq. (12) depicts the reaction at the protonated surface. All reaction products and stoichiometry are identified using X-ray spectroscopy (XAS) [8].

3.4. Kinetic study

3.4.1. Effect of contact time

Fig. 10 illustrates the As(III) removal rates as function of contact time at T = 308 K, S/L = 0.5% and $[As^{3+}]_0$ varies between 20–100 mg·L^{-1}.

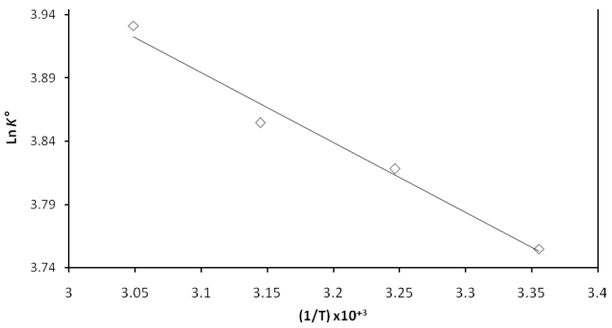

Fig. 8. The plot of ln$K°$ versus 1/T for As(III) adsorption on illite/Kaolinite clay.

Table 3
Thermodynamic constants for the adsorption of arsenite on illite + kaolinite at various temperatures (Time = 3h, $[As^{3+}]_0$ =20 mg·L^{-1} and S/L = 5 g·L^{-1})

T (K)	$\Delta G°$ (kJ·mol^{-1})	$\Delta H°$ (kJ·mol^{-1})	$\Delta S°$ (J·mol^{-1}·K^{-1})
298	–9.3	–4.588	15.8
308	–9.8		16.8
318	–10.2		17.6
328	–10.7		18.7

From this figure, we note that the adsorption rates are fairly high at the beginning and decline throughout the time. After 120 min, the reaction approaches equilibrium.

3.4.2. Effect of adsorbent dosage

The influence of adsorbent dosage in equilibrium uptake was studied at different initial concentrations $[As^{3+}]_0$ = 20, 40, 60, 80 and 100 mg·L^{-1}. As it can be noted from Fig. 11, the adsorption capacity of clay used decreases as the ratio Solid/Liquid increases, this is probably due to the creation of particles aggregation which reduces the specific surface area and leads to an increase in the diffusional path [19]. The second probable is due the reduction of the number of unsaturated sites [13]. Furthermore, as the amount of clay is increased, the pH of the medium increases, which affects the surface boundary and the arsenite speciation (see Fig. 9).

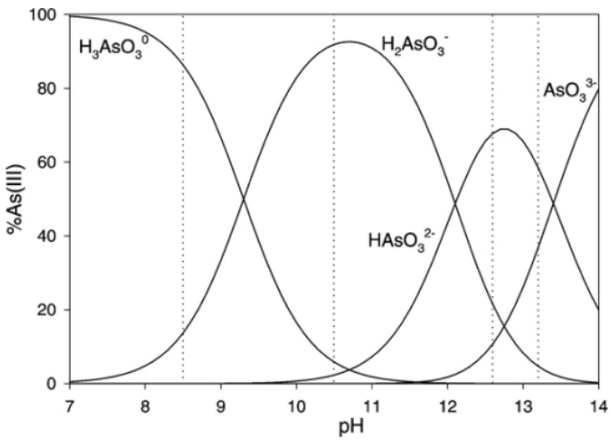

Fig. 9. Distribution of As(III) as a function of pH [4].

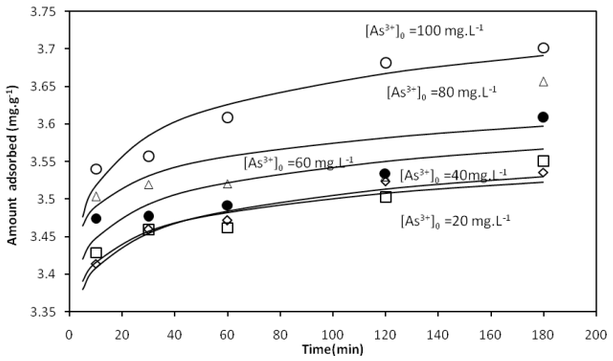

Fig. 10. The plot of As(III) removal rates against contact time at T = 308 K and absorbent dose 5 g·L^{-1}.

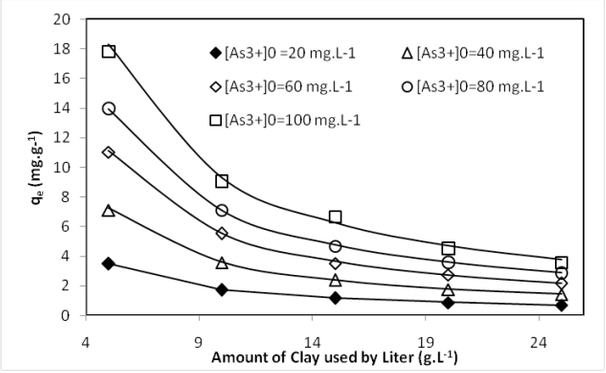

Fig. 11. Effect of clay used dosage on the adsorption capacity.

3.4.3. Adsorption modelling

Different models were used to investigate the kinetics of adsorbent-adsorbate interactions. The kinetics of As(III) adsorption from aqueous solutions using different types of clay material was well described by a pseudo-second order chemical reaction model [5,8–12,14,16,20]. All the earlier investigations noted that the pseudo-second order model assumes that the limiting step is the surface reaction. However, this model is unable to give others important adsorption parameters such mass transfer coefficient or effective pore diffusivity coefficient.

Studying the adsorption of As(III) on natural swelling clays (S_{BET} 25–140 m^2/g), Zehhaf et al. [5] attributed the change of basal spacing d_{001} before and after adsorption to the As (III) and As(V) diffusion into the inter-layers of clay and the mechanism embroiled in the adsorption could be investigated using intra-particle diffusion model [16]. In this work, the pseudo-second order model and the intra-particle model will be tested.

- *Pseudo second order reaction model*

  This model states that the adsorption capacity is proportional to the number of active sites on the surface. The differential equation is :

$$\frac{dq_i}{dt} = k_2\left(q_e - q_t\right)^2 \tag{13}$$

  The boundary conditions of this equation are: $t = 0 \rightarrow t \text{ and } q = 0 \rightarrow q_e$

  The rate law from Eq. (13) becomes:

$$\frac{1}{k_2 q_e^2} + \frac{t}{q_e} = \frac{t}{q_t} \tag{14}$$

where k_2 is the second order rate constant (g·mg^{-1}·min^{-1}); q_t (mg·g^{-1}) amount of adsorption at time t (min) and q_e (mg·g^{-1}) amount of adsorption at equilibrium.

By plotting t/qt versus t, we can determine the parameters k_2 and q_e from Eq. (14).

- *Intra particle diffusion control*

  The model is based on the Weber-Morris equation and described by:

$$q_e = k_{id} \times \sqrt{t} + c \tag{15}$$

where k_{id} is the interparticle diffusion rate constant (mg·g^{-1}·min$^{1/2}$) and c is a constant related to the thickness of the boundary layer.

The possibility of intra-particle transfer as a rate limiting step is confirmed by the straight line plots of q_e as function of $\sqrt{t}$ according to Eq. (15).

In Fig. 12, we represent the $\frac{q_{e,cal}}{q_{e,\exp}}$ ratio versus contact time for the pseudo-second-order model. As it can be seen from this figure, the beginning is not well fitted by this approach. Values of the mean root square error (MRSE) and the coefficient R^2 values are summarized in Table 4.

The value of the k_{id} was calculated from the slope of the linear plot of q_e versus $t^{1/2}$ (Fig. 13). It is clear from Fig. 13 that adsorption data of arsenite (III) onto the natural mixture of illite-kaolinite clay minerals fitted well in the interparticle model with high correlation coefficients and low RMSE at different S/L ratios. K_{id} lies between (1.1–1.8) × 10^{-2} mg·g^{-1}·min$^{-1/2}$. The fitted constants for the inter particle diffusion model are shown in Table 4.

4. Conclusion

Within the bounds of this study, naturally mixture illite + kaolinite clay mineral – mesoporous solid – proved to be effective for removing As(III) from aqueous solutions via adsorption technique. Experimental parameters such as contact time, adsorbent dose, initial arsenite concentration and temperature have been investigated and optimized. It is established that both ligand exchange and ion exchange at the surface may be the mechanism of adsorption. The maximum adsorption capacity was calculated by fitting Langmuir equation to the adsorption isotherms and found to be 233.1 mg·g^{-1} of clay and the Freundlich model was in good correlation with the adsorption isotherms data. The negative values of $\Delta G°$ and $\Delta H°$ reveal that the adsorption process is spontaneous and exothermic. The intra particle diffusion model was found to best correlate to our experimental data. The value of the intra particle diffusion rate constant K_{id} is about 0.012 mg·g^{-1}·min$^{-0.5}$. The results obtained in this work suggest that natural mixture of illite + kaolinite may provide the cost-reducing alternative to remove As(III) from groundwater and drinking water and to solve real problems in some countries.

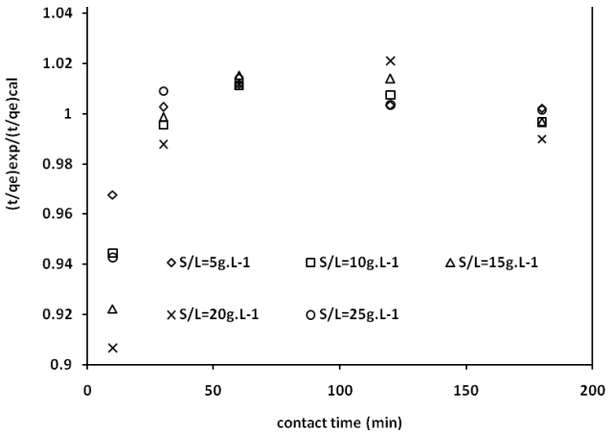

Fig. 12. Pseudo-second order representation at different solid/liquid ratios.

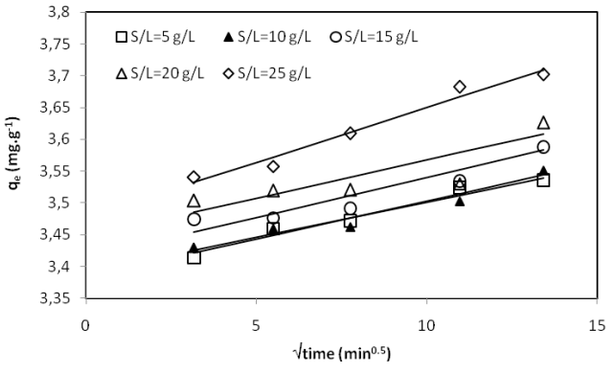

Fig. 13. Inter particle diffusion model at different solid/liquid ratios.

References

[1] Y. Bentahar, C. Hurel, K. Draoui, S. Khairoun, N. Marmier, Adsorptive properties of Moroccan clays for the removal of arsenic(V) from aqueous solution, Appl. Clay Sci., 119 (2016) 385–392.
[2] The Word Health Organization, Guidelines for Drinking-water Quality, vol.1. WHO, Geneva (1993).
[3] C.K. Jain, I. Ali, Arsenic: Occurrence, toxicity and speciation techniques, Water Res., 34(17) (2000) 4304–4312.
[4] M. Chibban, M. Zerbet, G. Carja, F. Sinan, Application of low-cost adsorbents for arsenic removal: A review, J. Environ. Chem. Ecotoxicol., 4(5) (2012) 91–102.
[5] A. Zehhaf, A. Benyoucef, C. Quijada, S. Taleb, E. Morallón, Algerian natural montmorillonites for arsenic(III) removal in aqueous solution, Int. J. Environ. Sci. Technol., 12(2) (2013) 595–602.
[6] K.P. Yadava, B.S. Tyagi, V.N. Singh, Removal of arsenic(III) from aqueous solution by china clay, Environ. Technol., 9 (1988) 1233–1244.
[7] M. Eloussaief, S. Bouaziz, N. Kallel, M. Benzina, Valorization of El Haria clay in the removal of arsenic from aqueous solution, Desal. Water Treat., 52 (2014) 2220–2224.
[8] A. Maiti, S. DasGupta, J.K. Basu, Sirshendu De, Adsorption of arsenite using natural laterite as adsorbent, Sep. Purif. Technol., 55(3) (2007) 350–359.
[9] M.D. Öztel, F. Akbal, L. Altaş, Arsenite removal by adsorption onto iron oxide-coated pumice and sepiolite, Environ. Earth Sci., 73 (2015) 4461–4471.
[10] K. Zhao, H. Guo, X. Zhou, Adsorption and heterogeneous oxidation of arsenite on modified granular natural siderite: Characterization and behaviors, Appl. Geochemistry, 48 (2014) 184–192.
[11] N. Ghorbanzadeh, W. Jung, A. Halajnia, A. Lakzian, A.N. Kabra, B.-H. Jeon, Removal of arsenate and arsenite from aqueous solution by adsorption on clay minerals, Geosystem Eng., 18(6) (2015) 302–311.

Table 4
Kinetic parameters for As(III) adsorption at different adsorbent doses

Pseudo-second order					Intra particle diffusion			
S/L Ratio	k_2 g·mg^{-1}·min^{-1}	q_e mg·g^{-1}	RMSE	R^2	k_{id} mg·g^{-1}·min$^{-1/2}$	Intercept mg·g^{-1}	RMSE	R^2
5 g·L^{-1}	0.364	3.55	0.021	0.999	0.01198	3.38	0.003	0.97
10 g·L^{-1}	0.284	3.55	0.033	0.999	0.01107	3.39	0.004	0.94
15 g·L^{-1}	0.211	3.62	0.046	0.999	0.01259	3.41	0.007	0.86
20 g·L^{-1}	0.184	3.64	0.056	0.998	0.01191	3.44	0.012	0.65
25 g·L^{-1}	0.227	3.73	0.034	0.999	0.01720	3.47	0.004	0.97

[12] P. Na, X. Jia, B. Yuan, Y. Li, J. Na, Y. Chen, L. Wang, Arsenic adsorption on Ti-pillared montmorillonite, J. Chem. Technol. Biotechnol., 85(5) (2010) 708–714.
[13] Y.W. You, H.T. Zhao, G.F. Vance, Removal of arsenite from aqueous solutions by anionic clays, Environ. Technol., 22(12) (2001) 1447–1457.
[14] T.A. Saleh, A. Sarı, M. Tuzen, Chitosan-modified vermiculite for As(III) adsorption from aqueous solution: Equilibrium, thermodynamic and kinetic studies, J. Mol. Liq., 219 (2016) 937–945.
[15] F. Bergaya, G. Lagaly, Purification of natural Clays, Developments in clay sci, 5 (2012) 213–221.
[16] N. Bektas, S. Aydin, M.S. Oncel, The adsorption of arsenic ions using beidellite, zeolite, and sepiolite clays: a study of kinetic, equilibrium, and thermodynamics, Sep. Sci. Technol., 46(6) (2011) 1005–1016.
[17] X. Zhou, X. Zhou, The unit problem in the thermodynamic calculation of adsorption using the Langmuir equation, Chem. Eng. Commun., 201(11) (2014) 1459–1467.
[18] A. Anjum, P. Lokeswari, M. Kaur, M. Datta, Removal of As(III) from aqueous solutions using montmorillonite, J. Anal. Sci. Meth. Instrum., 1, 25–30. Doi: 10.4236/jasmi. (2011), 12004.
[19] A. Sari, M. Tuzen, Ca(II) adsorption from aqueous solution by raw and modified kaolinite, Appl. Clay Sci., 88–89 (2014) 63–72.
[20] X. Ren, Z. Zhang, H. Luo, B. Hu, Z. Dang, C. Yang, L.L., Adsorption of arsenic on modified montmorillonite, Appl. Clay. Sci., 97–98 (2014) 17–23.